Formation of Star-Like and Linear Nanofibers via Controlled Crystallization of Poly(3-dodecylthiophene)

Zhongcheng Pan, Jing Ge, Hui Yang, Juan Peng, Feng Qiu

State Key Laboratory of Molecular Engineering of Polymers, Department of Macromolecular Science, Fudan University, Shanghai 200433, People's Republic of China
Correspondence to: J. Peng (E-mail: juanpeng@fudan.edu.cn)

Received 11 April 2013; revised 24 May 2013; accepted 28 May 2013; published online 22 June 2013
DOI: 10.1002/polb.23328

ABSTRACT: We report the crystalline behavior of poly(3-dodecylthiophene) (P3DDT) in aged toluene solution and link structure differences with the nature of seed nuclei related to various dissolution way. By directly stirring the P3DDT toluene solution for dissolution, the surviving fragments served as seed nuclei and star-like nanofibers were formed upon aging. While by heating the P3DDT solution for complete dissolution followed by cooling, the seed nuclei came from the π–π stacking of the planarized P3DDT chains and linear nanofibers were formed upon aging. Formation mechanisms and kinetics of different nanofibers are discussed in detail. © 2013 Wiley Periodicals, Inc. J. Polym. Sci., Part B: Polym. Phys. **2013**, *51*, 1268–1272

KEYWORDS: conjugated polymers; crystallization; fibers; nuclei; poly(3-dodecylthiophene)

INTRODUCTION Among conjugated polymers, poly(3-alkylthiophenes) (P3ATs) have received the most attention owing to their excellent charge carrier mobility, chemical stability, as well as facile preparation.[1] These superior characteristics make P3ATs widely used in organic electronics such as photovoltaic cells,[2–5] organic field-effect transistors,[6] and light-emitting diodes.[7] With a typical hair-rod molecular configuration, P3ATs can self-organize into semicrystalline nanofibers through strong anisotropic π–π interactions between planar rigid backbones and weak van der Waals interactions between their pendent alkyl side chains.[8] Well controlling the crystalline structure and morphology of P3ATs is important to improve the thin-film charge transport properties and the consequent device performance.

Up to now, great efforts have been made to control the crystalline structure of P3ATs. On the one hand, the size and crystalline structure of P3ATs can be controlled by post-treatment approach, such as application of electric field,[9] thermal, or solvent annealing.[10–14] On the other hand, the facile approach without post-treatment is more attractive, because the P3AT nanostructures can be well and directly tailored in solution systems by changing the solvent selectivity,[15] blending solvents,[16,17] ultrasonic treatment,[18,19] thermal treatment,[20] aging,[21,22] and so on. For example, by adding a small amount of the nonsolvent acetonitrile to the P3HT precursor solution, the crystallinity of the P3HT thin films is significantly increased with a field-effect mobility dramatically improved without post-treatment.[23] Using the combined centrifugation–filtration method, the P3HT fibers can be separated from the well-dissolved P3HT chains and a maximum power conversion efficiency of 3.6% has been achieved in solar cell performance with an optimum composition between nanofibers and disorganized P3HT.[24]

In general, two steps are involved in P3AT crystallization from solution: coil-to-rod conformational transition followed by π–π stacking of the rod-like polymer chains.[16] In a typical procedure which is called whisker method, P3ATs were first dissolved in their marginal solvents with heating and cooled to room temperature to form nanofibers.[25,26] A great deal of characterization of P3AT nanofibers has been performed based on the whisker method. However, very few researchers have investigated the effect of various dissolution ways of P3ATs on the nanofiber formation.[27] In particular, the nature of seed nuclei related to the dissolution procedure has a large effect on the crystalline morphology of P3ATs and is therefore an important aspect to control.

Here, we report the crystalline behavior of poly(3-dodecylthiophene) (P3DDT) in aged toluene solution. By directly stirring the P3DDT toluene solution for dissolution, the surviving fragments served as seed nuclei and star-like nanofibers were formed upon aging. While by heating the P3DDT

Additional Supporting Information may be found in the online version of this article.

solution for complete dissolution followed by cooling, the seed nuclei came from the π–π stacking of the planarized P3DDT chains and linear nanofibers were formed upon aging. The results revealed that the nature of P3DDT seed nuclei not only affected the morphology and length of nanofibers, but also determined the kinetics of nanofiber formation in the aged process. This study correlates the dissolution way with the nature of P3DDT seed nuclei, which can improve our understanding of various P3DDT crystalline behaviors.

EXPERIMENTAL

Preparation of P3DDT Nanofiber Solution

P3DDT (M_n = 17,000 g/mol, M_w/M_n = 1.23) was synthesized by a modified Grignard metathesis method.[28] Two methods were used to dissolve the P3DDT in toluene (1.0 mg/mL). Method 1: P3DDT was dissolved into toluene by stirring overnight at room temperature. Importantly, the solubility of P3DDT in toluene without heating remained sufficiently high, which was confirmed by visibly clear solution without noticeable polymer aggregates. Method 2: P3DDT was dissolved into toluene by heating at 80 °C overnight for complete dissolution and cooled to room temperature. The solutions prepared by the two methods were aged for different times for the crystallization of P3DDT and growth of nanofibers.

Characterization

Atomic force microscopy (AFM) was performed at ambient conditions by a commercial AFM, using a Digital Instruments MultiMode IV in the tapping mode. The dry samples were mounted on a sample stage which was three-dimensionally driven by a piezo tube scanner. Both height and phase images were recorded simultaneously. The samples for AFM were spin-coated from their solutions onto the precleaned silicon substrates at 3000 rpm for 60 s. Prior to spin-coating, the wafers were cleaned with a 70/30 v/v solution of 98% H_2SO_4/30% H_2O_2 at 80 °C for 30 min, and then thoroughly rinsed with deionized water and dried.

Transmission electron microscopy (TEM) was taken on a Tecnai G^2 20, FEI electron microscope operated at 200 kV. As for TEM analysis, the samples were prepared by drop-casting their solutions onto carbon-coated copper grids, followed by evaporation of the solvent at ambient.

X-ray diffraction (XRD) was performed on a PANalytical X'Pert PRO X-ray diffractometer using Cu Kα radiation (λ = 1.541 Å) operating at 40 kV and 40 mA. The film samples for XRD measurements were prepared by drop-casting their solutions onto silicon substrates and dried before measurements. The powder samples were prepared by evenly spreading the P3DDT powder onto a silicon holder before measurements.

UV–vis spectroscopy was carried out with a Perkin-Elmer Lambda 35 equipment. To avoid signal saturation, the P3DDT concentration in UV–vis was diluted to 0.5 mg/mL.

RESULTS AND DISCUSSION

Figure 1(a–d) shows the growth process of P3DDT star-like nanofibers from the aged solution. After directly stirring the P3DDT toluene solution for dissolution, the thin-film spin-coated from the freshly prepared solution (aged for 0 day) showed some grains with most diameters ranging from ~100 to 250 nm [Fig. 1(a)]. Although without heating, P3DDT readily dissolved in toluene and formed free polymer chain owing to its long alkyl side chains. The grains that survived the dissolution procedure served as seed nuclei for further P3DDT crystallization during aging process. Aged for 0.5 day, some branches grew onto these grains in all

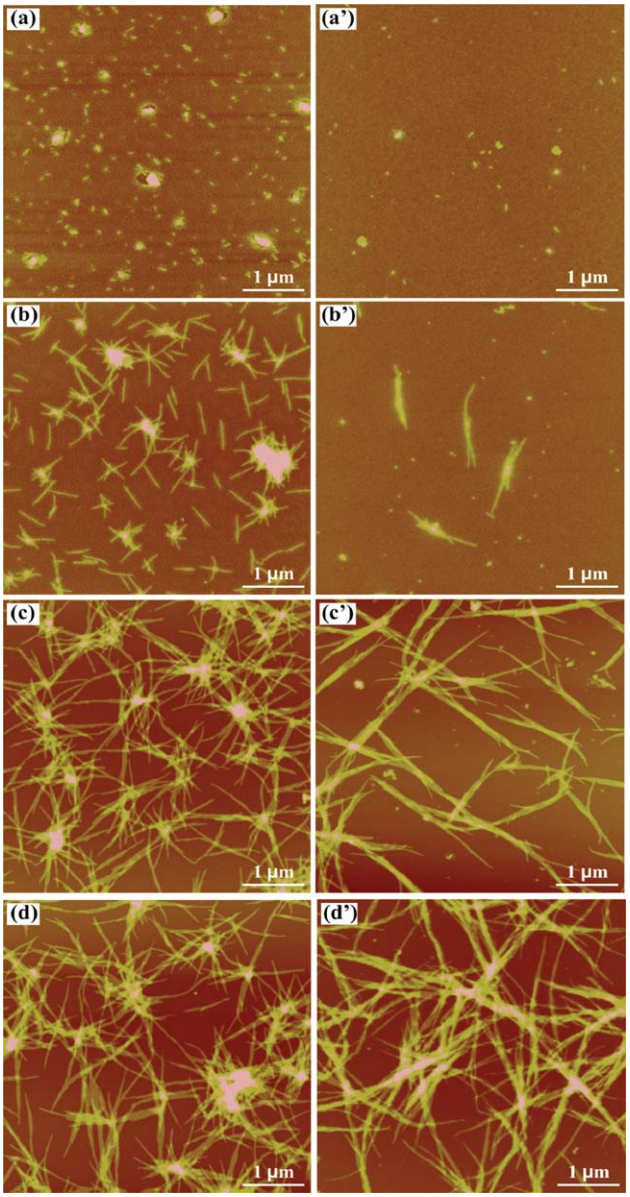

FIGURE 1 AFM images showing the growth process of (a–d) P3DDT star-like nanofibers and (a'–d') P3DDT linear nanofibers spin-coated from different freshly prepared solutions and aged for different times. (a) 0, (b) 0.5, (c) 1, and (d) 2 days. (a') 0, (b') 1, (c') 6, and (d') 10 days.

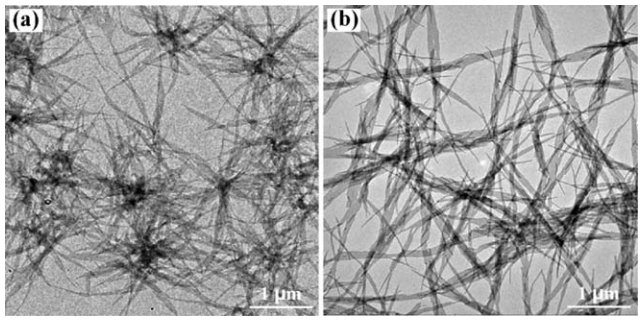

FIGURE 2 TEM images of (a) P3DDT star-like nanofiber solution aged for 2 days and (b) P3DDT linear nanofiber solution aged for 10 days.

directions, with the width, height, and length of ~75, 7, and 300–500 nm, respectively [Fig. 1(b)]. As increased aging time, these branches gradually grew into longer nanofibers with the length of 0.5–1.2 μm, leading to star-like structures [Fig. 1(c,d)]. The star-like nanofibers did not further grow after aging for 5 days, indicating that P3DDT crystallization was complete.

Next, we will show that the growth process of P3DDT linear nanofibers [Fig. 1(a'–d')], which is different from that of star-like nanofibers at the beginning of the freshly prepared solution. After heating the P3DDT solution for complete dissolution and cooling process, much less seed nuclei were observed on the spin-coated thin film compared with that from directly stirred P3DDT solution [Fig. 1(a')]. With the increased aging time for 1 day, some short nanorods appeared with the width, height, and length of ~80, 7, and 1–1.5 μm, respectively [Fig. 1(b')]. After an extended duration of aging (6 days), these nanorods gradually grew into longer one-dimensional linear nanofibers with the length of 2.5–5 μm and connected with each other [Fig. 1(c')]. The P3DDT crystallization was complete after aging for 10 days, much longer than the case of star-like nanofibers [Fig. 1(d')]. Plan-view TEM images of the solutions of Figure 1(d,d') are shown in Figure 2. The consistent morphology measured by TEM and AFM indicated the dry AFM sample represented the case in the solution.

The crystalline structures of the P3DDT star-like nanofibers and linear nanofibers were characterized using XRD [Fig. 3(a)]. Both of the samples showed a recognizable diffraction peak at $2\theta = 3.7^\circ$ assigned to the (100) reflection of the P3DDT chains with a d-spacing of 23.8 Å. The emergence of (100) diffraction peak suggested that the P3DDT molecules adopt an "edge-on" orientation in both star-like and linear nanofibers, where the direction of π–π stacking and the layers of P3DDT side chains were parallel and perpendicular to the substrate, respectively [Fig. 3(b)]. Considering the height of the nanofibers (~7 nm), there are approximately three layers of P3DDT backbones laminating perpendicular to the long axis of the nanofibers.

It is known that P3AT crystallization involves two steps, that is, coil-to-rod conformational transition followed by crystallization of the rods. The first process is controlled by the activation energy of conformational change (ΔF), whereas the second process is determined by the free energy change for the formation of critical size nucleus (ΔG).[21] For P3DDT, ΔF and ΔG are ~35 and 31.8 kcal/mol, respectively.[29] Therefore, the decisive factor for the crystalline process of P3DDT in toluene is the coil-to-rod conformation transition. The formation of star-like or linear nanofibers during aging proved that P3DDT molecules could overcome the barrier of coil-to-rod transition in both cases.

With respect to the reason for the formation of different star-like and linear nanofiber morphology, the origin and nature of the seed nuclei were different in the two cases,

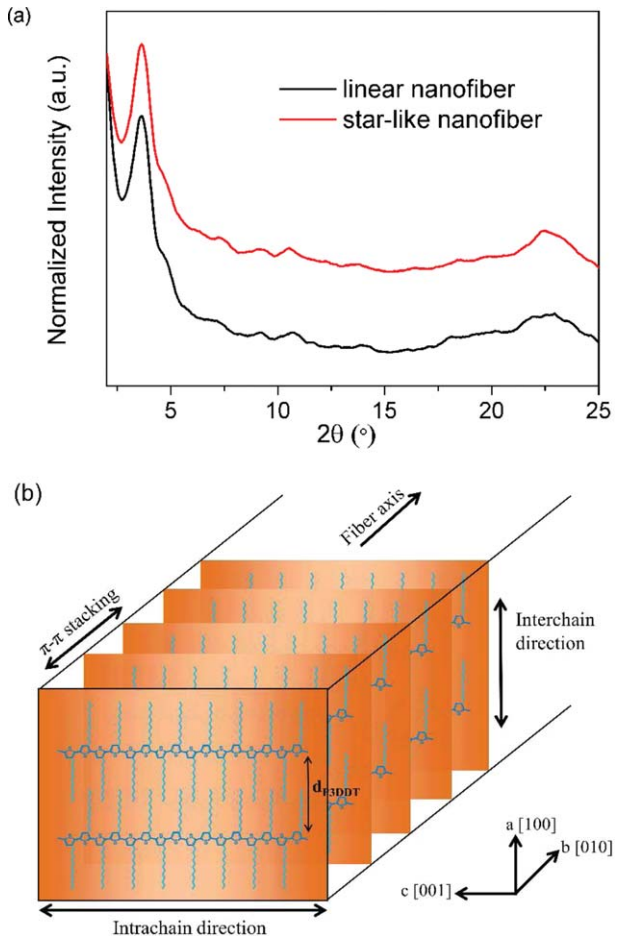

FIGURE 3 (a) XRD profiles of the thick films drop-cast from P3DDT star-like nanofiber solution aged for 2 days and linear nanofiber solution aged for 10 days. (b) Schematic illustration of the P3DDT molecular arrangement, corresponding to an "edge-on" orientation in both star-like and linear nanofibers.

which determined the growth of P3DDT nanofibers in different way. By directly stirring the P3DDT toluene solution without heating, most of the P3DDT chains were dissolved and the surviving fragments served as seed nuclei for further P3DDT crystallization in the case of star-like nanofibers.

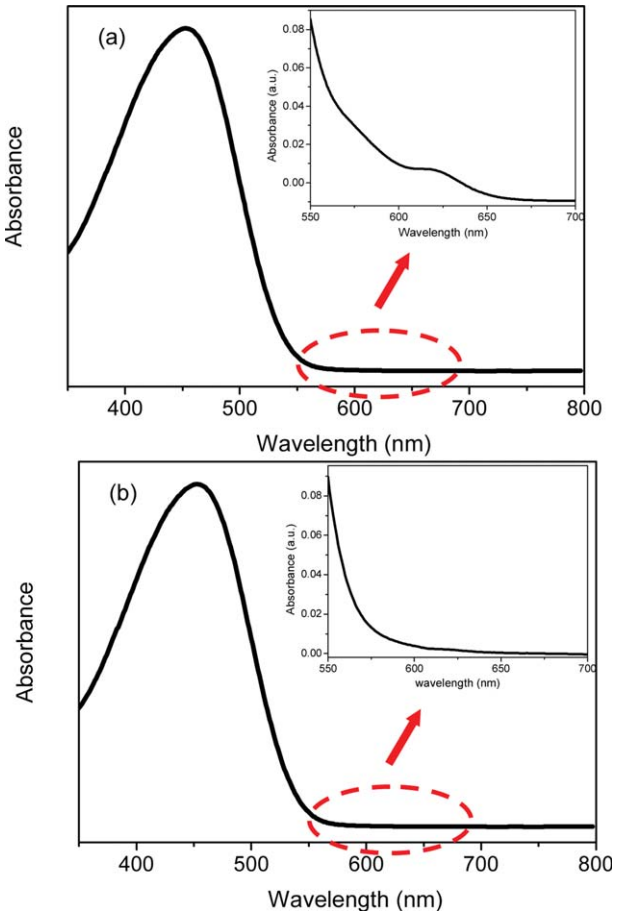

FIGURE 4 UV–vis absorption spectra of freshly prepared P3DDT toluene solution via (a) stir-induced dissolution and (b) heating–cooling process.

Based on the XRD results (Supporting Information Fig. S1), the crystalline structure existed in the P3DDT powder before dissolution. Furthermore, the surviving component was more perfect crystallites compared with the dissolved part upon dissolution.[30] As a result, it was assumed that these seed nuclei were crystalline which could be further proved by UV–vis. It is well known that if P3AT forms ordered aggregates, an absorption peak centered at about 610 nm will appear in its UV–vis absorption spectrum.[31–33] In this case, the appearance of the low-energy absorption at 610 nm indicated the crystalline aggregates in the solution (Fig. 4(a), inset). The crystalline planes were assumed to be randomly located on the seed nuclei. As the solution was aged, the P3DDT molecules in solution crystallized onto these crystalline planes to form branches. In other words, the existed crystalline planes on the seed nuclei guided the growth direction of followed P3DDT crystallization. With the increased aging time, these P3DDT branches gradually grew into longer nanofibers in all direction to form star-like nanofibers.

Although in the case of linear nanofibers, the P3DDTs were completely dissolved by heating and adopted a coil-like conformation. Upon cooling, a few chains gradually changed their conformation to planar conformation and π–π stacking of the conjugated P3DDT occurred, resulting in the crystalline seed nuclei. The absorption at 610 nm was almost invisible in UV–vis owing to small amount of seed nuclei (Fig. 4(b), inset). These seed nuclei came from the π–π stacking of the planarized P3DDT chains with the crystalline planes located only at both ends of them, which guided the P3DDT crystallization onto these planes in one-dimension to form linear nanofibers. The formation process of star-like and linear nanofibers is schematically shown in Figure 5.

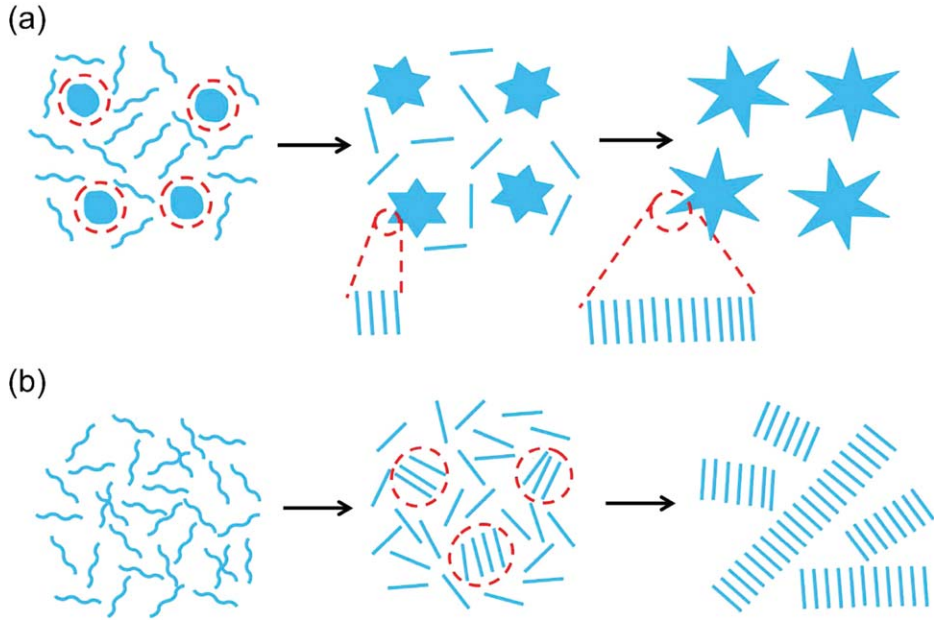

FIGURE 5 Schematic illustration showing the growth process of (a) P3DDT star-like nanofibers and (b) linear nanofibers.

Our experimental observation revealed that the final length of nanofibers depended strongly on the number and nature of seed nuclei present at the beginning and it decreased with the increased number of seed nuclei (Fig. 1). On the one hand, the more seed nuclei lead the more P3DDT molecules crystallize onto them at the same time. On the other hand, as far as one single-seed nucleus, the more crystalline planes guide the more P3DDT molecules crystallize onto them at the same time. Both the number of seed nuclei and the crystalline planes on one single-seed nucleus were much more in the case of star-like nanofibers than those of linear nanofibers. Therefore, the length of star-like nanofibers was shorter than that of linear nanofibers. In addition, as more P3DDT molecules were consumed at the same time to form star-like nanofibers, the kinetics of P3DDT crystallization was much faster in the formation of star-like nanofibers than that of linear nanofibers.

CONCLUSIONS

In summary, we wish to mention that stirring or heating is generally used in P3AT nanofiber preparation. However, to the best of our knowledge, their independent contribution to the nanofiber formation is seldom investigated. The nature of P3DDT seed nuclei was related to the dissolution way, which yielded star-like or linear nanofibers in the aging process. The P3DDT seed nuclei survived from stir-induced dissolution were crystallized with randomly located crystalline planes, which guided the following P3DDT crystallization on these planes to form branches in all direction and finally grew into star-like nanofibers. While during heating–cooling process, the seed nuclei came from the π-π stacking of the planarized P3DDT chains with crystalline planes only located at both ends of the seed nuclei. The P3DDT molecules crystallized onto these planes in one-dimension and gradually grew into long linear nanofibers. This study may offer an effective way to improve the understanding of various P3DDT crystalline behaviors and facilitate the ongoing exploration of the nature of seed nuclei as an influencing factor on the nanofiber formation.

ACKNOWLEDGMENTS

This study was financially supported by the National Natural Science Foundation of China (Grant No. 21074026, 21274029 and 20990231) and National Basic Research Program of China (2011CB605700).

REFERENCES AND NOTES

1 Y. J. Cheng, S. H. Yang, C. S. Hsu, *Chem. Rev.* **2009**, *109*, 5868–5923.

2 G. Li, V. Shrotriya, J. S. Huang, Y. Yao, T. Moriarty, K. Emery, Y. Yang, *Nat. Mater.* **2005**, *4*, 864–868.

3 G. Q. Ren, P. T. Wu, S. A. Jenekhe, *Chem. Mater.* **2010**, *22*, 2020–2026.

4 H. J. Wang, Y. P. Chen, Y. C. Chen, C. P. Chen, R. H. Lee, L. H. Chan, R. J. Jeng, *Polymer* **2012**, *53*, 4091–4103.

5 M. Lanzi, L. Paganin, F. Errani, *Polymer* **2012**, *53*, 2134–2145.

6 R. J. Kline, M. D. McGehee, M. F. Toney, *Nat. Mater.* **2006**, *5*, 222–228.

7 R. Osterbacka, G. Juska, K. Arlauskas, A. J. Pal, K. M. Kalman, H. Stubb, *J. Appl. Phys.* **1998**, *84*, 359.

8 H. Yan, Y. Yan, Z. Yu, Z. Wei, *J. Phys. Chem. C* **2011**, *115*, 3257–3262.

9 R. A. Marsh, J. M. Hodgkiss, R. H. Friend, *Adv. Mater.* **2010**, *22*, 3672–3676.

10 J. Ge, M. He, X. B. Yang, Z. Ye, X. Liu, F. Qiu, *J. Mater. Chem.* **2012**, *22*, 19213–19221.

11 Z. J. Gu, T. Kanto, K. Tsuchiya, T. Shimomura, K. Ogino, *J. Polym. Sci. Part A: Polym. Chem.* **2011**, *49*, 2645–2652.

12 Y. Zhao, Z. Y. Xie, Y. Qu, Y. H. Geng, L. X. Wang, *Appl. Phys. Lett.* **2007**, *90*, 043504.

13 D. H. Kim, Y. D. Park, Y. Jang, S. Kim, K. Cho, *Macromol. Rapid Commun.* **2005**, *26*, 834–839.

14 G. Lu, L. G. Li, X. N. Yang, *Adv. Mater.* **2007**, *19*, 3594–3598.

15 J. D. Roehling, I. Arslan, A. J. Moule, *J. Mater. Chem.* **2012**, *22*, 2498–2506.

16 M. He, L. Zhao, J. Wang, W. Han, Y. L. Yang, F. Qiu, Z. Q. Lin, *ACS Nano* **2010**, *4*, 3241–3247.

17 W. Xu, L. Li, H. Tang, H. Li, X. Zhao, X. N. Yang, *J. Phys. Chem. B* **2011**, *115*, 6412–6420.

18 K. Zhao, L. J. Xue, J. G. Liu, X. Gao, S. P. Wu, Y. C. Han, Y. H. Geng, *Langmuir* **2010**, *26*, 471–477.

19 S. K. Patra, R. Ahmed, G. R. Whittell, D. J. Lunn, E. L. Dunphy, M. A. Winnik, I. Manners, *J. Am. Chem. Soc.* **2011**, *133*, 8842–8845.

20 Y. Huang, H. Cheng, C. C. Han, *Macromolecules* **2010**, *43*, 10031–10037.

21 L. J. Xue, X. Gao, K. Zhao, J. G. Liu, X. H. Yu, Y. C. Han, *Nanotechnology* **2010**, *21*, 145303.

22 Y. D. Park, S. G. Lee, H. S. Lee, D. Kwak, D. H. Lee, K. Cho, *J. Mater. Chem.* **2011**, *21*, 2338–2343.

23 Y. D. Park, H. S. Lee, Y. J. Choi, D. Kwak, J. H. Cho, S. Lee, K. Cho, *Adv. Funct. Mater.* **2009**, *19*, 1200–1206.

24 S. Berson, R. De. Bettignies, S. Bailly, S. Guillerez, *Adv. Funct. Mater.* **2007**, *17*, 1377–1384.

25 S. Samitsu, T. Shimomura, S. Heike, T. Hashizume, K. Ito, *Macromolecules* **2008**, *41*, 8000–8010.

26 M. He, J. Ge, M. Fang, F. Qiu, Y. L. Yang, *Polymer* **2010**, *51*, 2236–2243.

27 J. Y. Oh, M. Shin, T. I. Lee, W. S. Jang, Y. Min, J. M. Myoung, H. K. Baik, U. Jeong, *Macromolecules* **2012**, *45*, 7504–7513.

28 J. Ge, M. He, F. Qiu, Y. L. Yang, *Macromolecules* **2010**, *43*, 6422–6428.

29 S. Malik, A. K. Nandi, *J. Appl. Polym. Sci.* **2007**, *103*, 2528–2537.

30 J. S. Qian, G. Guerin, Y. J. Lu, G. Cambridge, I. Manners, M. A. Winnik, *Angew. Chem. Int. Ed.* **2011**, *50*, 1622–1625.

31 Z. C. Pan, J. Ge, W. H. Li, J. Peng, F. Qiu, *Soft Matter* **2012**, *8*, 9981–9984.

32 L. G. Li, H. W. Tang, H. X. Wu, G. H. Lu, X. N. Yang, *Org. Electron.* **2009**, *10*, 1334–1344.

33 T. Yamamoto, D. Komarudin, M. Arai, B. L. Lee, H. Suganuma, N. Asakawa, Y. Inoue, K. Kubota, S. Sasaki, T. Fukuda, H. J. Matsuda, *J. Am. Chem. Soc.* **1998**, *120*, 2047–2058.